



OPEN ACCESS

EDITED BY
Han Pu,
Rice University, United States

REVIEWED BY
Zbigniew Łaszczysz, Wrocław University of Technology, Poland
Jingjing Zheng, Beijing Jiaotong University, China

*CORRESPONDENCE
Pan Zhang,
✉ zhangpan@ntsc.ac.cn

SPECIALTY SECTION
This article was submitted to Atomic and Molecular Physics, a section of the journal Frontiers in Physics

RECEIVED 18 October 2022
ACCEPTED 06 December 2022
PUBLISHED 16 December 2022

CITATION
Rao B, Li M, Yang X, Yan L, Chen X, Yuan R, Zhang P and Zhang S (2022), Polarization-multiplexed dual-comb fiber laser based on an all-polarization-maintaining cavity configuration. *Front. Phys.* 10:1073201. doi: 10.3389/fphy.2022.1073201

COPYRIGHT
© 2022 Rao, Li, Yang, Yan, Chen, Yuan, Zhang and Zhang. This is an open-access article distributed under the terms of the [Creative Commons Attribution License \(CC BY\)](https://creativecommons.org/licenses/by/4.0/). The use, distribution or reproduction in other forums is permitted, provided the original author(s) and the copyright owner(s) are credited and that the original publication in this journal is cited, in accordance with accepted academic practice. No use, distribution or reproduction is permitted which does not comply with these terms.

Polarization-multiplexed dual-comb fiber laser based on an all-polarization-maintaining cavity configuration

Bingjie Rao^{1,2}, Mingkun Li^{1,2}, Xiguang Yang^{1,2}, Lulu Yan¹, Xin Chen^{1,2}, Ru Yuan^{1,2}, Pan Zhang^{1,3*} and Shougang Zhang^{1,2}

¹National Time Service Center, Chinese Academy of Sciences, Xi'an, China, ²School of Astronomy and Space Science, University of Chinese Academy of Sciences, Beijing, China, ³State Key Laboratory of Transient Optics and Photonics, Chinese Academy of Sciences, Xi'an, China

In this study, we present a polarization-multiplexed, erbium-doped dual-comb fiber laser based on an all-polarization-maintaining cavity configuration. We observed that the dual-comb fiber laser easily realized the self-starting mode-locking operation due to the non-linear amplifying loop mirror (NALM) with a non-reciprocal phase shifter. Furthermore, owing to the sharing of the NALM part, the two outputs from this laser configuration had similar center wavelengths, with small different repetition rates (Δf_{rep}). In the free-running operation, the standard deviation of relative stability for Δf_{rep} of 2.09 kHz was measured to be 1.59 Hz, and the full width at half-maximum of the relative beat note between the two frequency combs in the optical frequency domain was approximately 1 kHz. These results show that the two frequency combs from this laser configuration have high relative stability and mutual coherence.

KEYWORDS

erbium fiber-based femtosecond optical frequency comb, dual-comb fiber laser, mode-locked laser, non-linear amplifying loop mirror, dual-comb spectroscopy

1 Introduction

As a simple and efficient optical frequency measurement tool, the optical frequency comb (OFC) can directly realize frequency measurements by converting optical frequency into radiofrequency (RF). With its advantages, it has been widely applied in astronomical spectrograph calibrations [1–3], stable microwave generation [4–6], precision laser frequency spectroscopy [7–9], and precision distance measurements [10, 11]. Studies have also reported that fiber-based OFCs using a polarization-maintaining fiber (PMF) offer an inexpensive, compact, and robust setup by decoupling the laser part, thereby reducing environmental perturbations. Moreover, in these lasers, a mode-locking mechanism using a semiconductor saturable absorber mirror (SESAM) is commonly applied because of its easy combination with PMF and self-starting mode-locking operation [12–14]. However, owing to the SESAM's intrinsic effects, such as its slow lifetime, only SESAM-based fiber lasers' relative intensity noise level can worsen compared to the other mode-locking mechanisms [15, 16]. In contrast, a PMF mode-

locked laser based on a non-linear amplifying loop mirror (NALM) has been identified. Although it often introduces an intrinsic non-reciprocal device for self-starting mode-locking operations, it has a low noise capability because of its inherent amplitude noise suppression caused by artificial saturable absorber mechanism [17–19].

Dual-comb spectroscopy (DCS) is a common measuring technique uses mechanically scan-less Fourier transform that was first proposed by Schiller in 2002 and then experimentally confirmed by Keilmann in 2004 [20, 21]. Due to its various advantages compared with other techniques in acquisition time, sensitivity and resolution, DSC is attracting wide attention [20, 22]. The essence of DCS is the use of two frequency combs with slightly different repetition rate (Δf_{rep}) to achieve a spectral resolution. Universally, two independent femtosecond mode-locked lasers whose repetition frequency (f_{rep}) and carrier-envelope-offset frequency (f_{ceo}) are tightly phase-locked to a reference source, such as a stable continuous wave laser, are involved in a conventional DCS setup [23–25]. With this configuration, a nearly ideal dual-comb system whose comb teeth have extremely narrow linewidth and precise frequency in the broadband range is obtained for high-resolution and wide-bandwidth spectroscopy. However, the conventional DCS requires a complex phase-locked feedback control, leading to extremely high complexity and cost, making further applications in systems with strict limitations, such as volume and power consumption, difficult.

Due to its high performance and low cost, a dual-comb fiber laser without complex tight phase locking, which can emit asynchronous pulses, has attracted the interests of researchers [26–37]. Interestingly, since this free-running single-cavity fiber laser possesses common mode noise suppression, its relative stability and mutual coherence are considerably high. Therefore, conducting an active servo control has become unnecessary, significantly reducing the complexity and cost. This simple and efficient laser has the potential to simplify DCS setups. Based on this principle, various dual-comb fiber lasers depending on wavelength division multiplexing [26–28], bidirectional scheme [29–32], polarization multiplexing [33–36], and pulse shape multiplexing [37] have been sufficiently developed. Studies have also focused on all-polarization-maintaining (PM) dual-comb fiber lasers based on the NALM mode-locking mechanism. In these lasers, spectral filtering schemes, such as using a Lyot filter, a Sagnac filter, and a spectral filter, are always employed to generate two frequency combs [38–40]. Still, owing to the different center wavelengths in the two frequency combs, an additional spectral broadening is deemed necessary for practical application [34]. Besides, polarization-multiplexed and mechanical sharing schemes have been reported for all-PM dual-comb fiber lasers with NALM. However, the laser configuration of these dual-comb fiber lasers is considered complex for a practical DCS [34, 41].

Given the facts above, this study was able to develop an all-PM polarization-multiplexed, dual-comb fiber laser employing the NALM mode-locking mechanism. This developed dual-comb fiber laser easily realized the self-starting mode-locking operation by employing a non-reciprocal phase shifter. As a result, the dual-comb fiber laser emitted asynchronous outputs at similar center wavelengths due to the small difference in intracavity losses between the two frequency combs. In the free-running operation, a standard deviation of 1.59 Hz was obtained for a small Δf_{rep} of 2.09 kHz, and a full width at half-maximum of approximately 1 kHz was obtained for a relative beat note. This simple, robust, turnkey laser configuration is a promising tool in practical DCS.

2 Experimental setup

The schematic showing the polarization-multiplexed, Er-doped dual-comb fiber laser based on an all-PM cavity configuration is illustrated in Figure 1. The mode-locking mechanism of our dual-comb fiber laser was based on NALM, which is similar to the laser configuration described in (18). This laser comprised two linear arms based on free space and an NALM part based on fiber and free space. Notably, all the fiber components in the laser were PM, which highly improved the robustness of the laser. The NALM part comprised a 980 nm/1,550 nm wavelength division multiplexer (WDM), a 160-cm-long non-doped PMF, an 80-cm-long Er-doped PMF (EDF, Liekki, Er80-4/125/HD), a polarization beam splitter (PBS), two fiber collimators (COs), two half-waveplates (HWPs), and two 976 nm laser diodes (CM97-1000-76PM, II-VI) coupled by a pump combiner. In the fiber components of the NALM part, both polarization axes in a PMF were used for dual-comb generation. HWPs were used for finely tuning the splitting ratio of PBS1 and ensuring horizontally or vertically polarized component propagated along the fast or slow axis. By changing the angular orientation of the HPWs, the propagating axis of comb1 and comb2 was fast and slow axes, respectively. Furthermore, each linear arm comprised a 45° Faraday rotator (FR), an eighth-waveplate (EWP), a PBS, and a mirror (M), respectively. The non-reciprocal phase shifter comprised an FR and EWP placed between the PBS1 and PBS2, which reduced the mode-locking threshold of the laser and assisted the self-starting mode-locking operation. In each linear arm, a displacement stage placed under the M was employed to adjust the cavity length of the comb1 or comb2, and a fiber collimator (CO) (not shown in Figure 1) placed on the reflect port of the PBS2 was employed to couple the output (comb1 or comb2) of the laser to a PMF.

As we have evaluated the net dispersion of the dual-comb fiber laser to be -0.01 ps^2 at 1,550 nm. All the non-common components were placed closely on the same platform to share the mechanical vibrations. Additionally, in order to isolate environmental

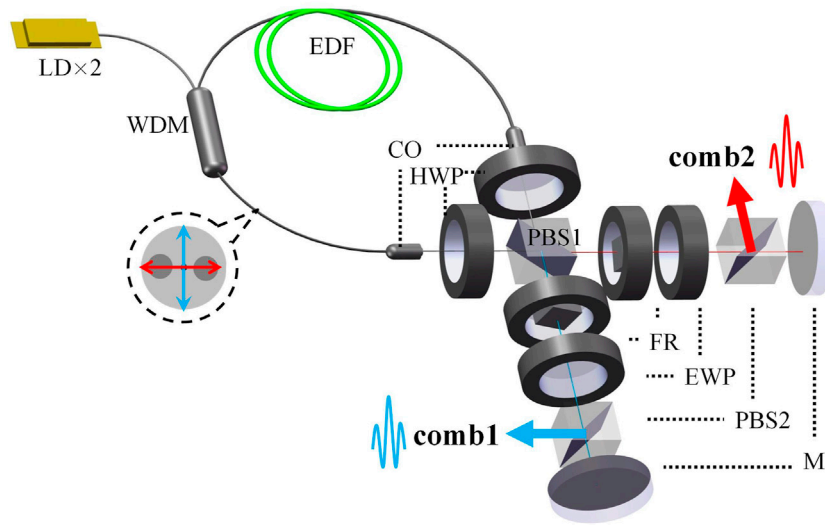


FIGURE 1
Schematic showing the polarization-multiplexed dual-comb fiber laser based on the all-polarization-maintaining cavity configuration. LD, laser diode; EDF, Er-doped fiber; CO, fiber collimator; WDM, wavelength division multiplexer (980 nm/1,550 nm); PBS, polarization beam splitter; HWP, half-wave plate; EWP, eighth-wave plate; FR, Faraday rotator; M, mirror.

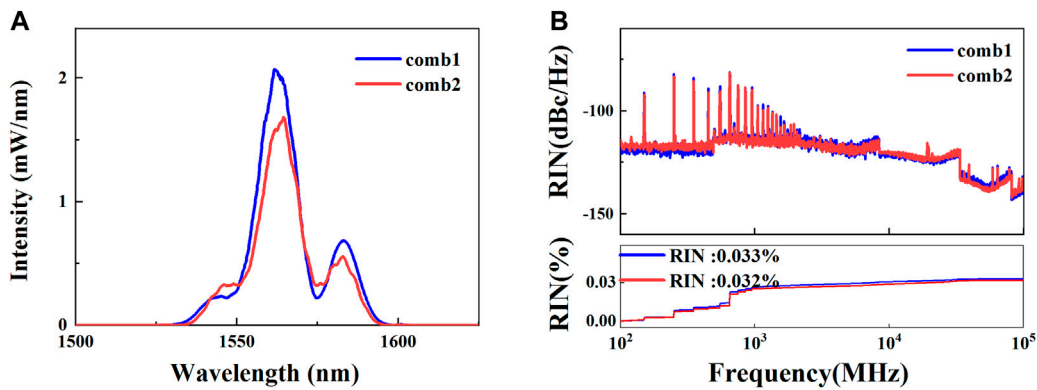
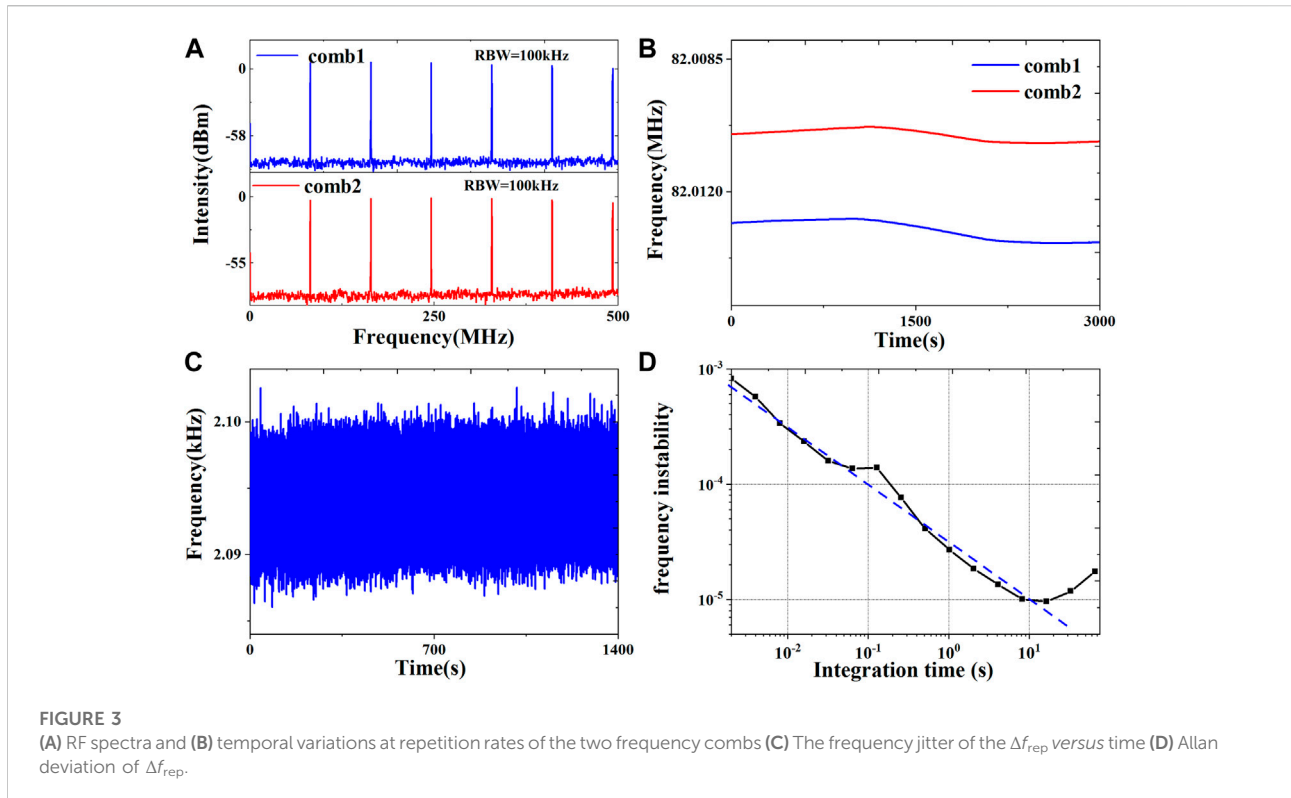


FIGURE 2
(A) Optical spectra and (B) RIN curves of the two frequency combs.

disturbance, all components of the laser were placed in a simple box. As a result, when the pump power increased, the dual-comb fiber laser could easily realize self-starting mode-locking operation, owing to using a non-reciprocal phase shifter. Furthermore, by adjusting the position of the displacement stage, Δf_{rep} between the two frequency combs was finely tuned from 10 kHz to 10 Hz. The tunable Δf_{rep} could provide a flexible spectral range for practical DCS, and Δf_{rep} was as low as ~ 10 Hz, which maximally providing about 336 THz bandwidth before the two frequency combs alias. All experiments and results in this paper were completed in the free-running operation.

3 Results and discussion

It was observed that the lower Δf_{rep} value was, the lower pump power was required for mode-locking operation. When the Δf_{rep} was ~ 2 kHz, the dual-comb fiber laser could realize the self-starting mode-locking operation at the pump power rose to 890 mW, and then realized a single-pulse mode-locking operation at the pump power dropped down to 700 mW. The optical spectra of the dual-comb fiber laser outputs measured by an optical spectrum analyzer (YOKOGAWA, AQ6375B) are shown in Figure 2A [comb1 (blue) and comb2 (red)] at a pump power of 670 mW. The center

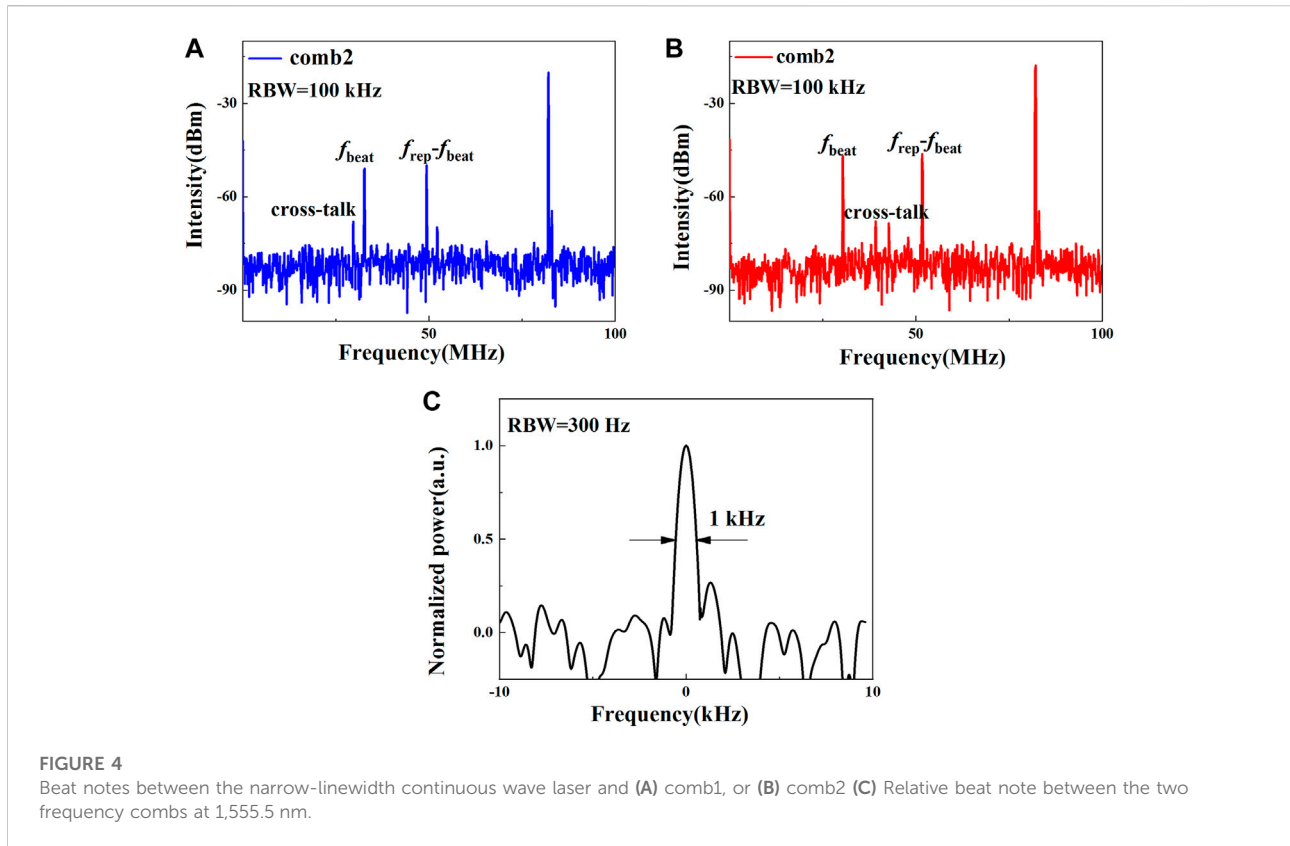


wavelength, full width at half-maximum (FWHM) bandwidth of the spectrum, and output power of comb1 were 1,562.5 nm, 13.4 nm, and 39.2 mW, respectively. Correspondingly, the center wavelength, FWHM, and output power of comb2 were 1,563.3 nm, 13.1 nm, and 33.5 mW, respectively. Notably, the spectral shape didn't show the typical characteristics of stretched pulses, due to the interference of two counter-propagating beams at the PBS2. The measured optical spectrum was the reflected polarization component of intra-cavity pulse and was related to the phase bias introduced by the non-reciprocal phase shifter [42–44]. Moreover, due to the difference in intra-cavity losses between the two frequency combs, a slight difference in the optical spectra and output powers was also observed from Figure 2A, which could be further optimized by improving the coupling of the free space.

The intensity noise of a laser mainly comes from quantum noise (spontaneous emission noise and shot noise) and external technical noise (pump laser source noise). It indirectly affects the performance of an OFC system by noise coupling [45–47]. In order to evaluate the relative intensity noise (RIN) of the dual-comb fiber laser, the output (comb1 or comb2) of the laser was coupled into a photodetector (Thorlabs, PDA20CS-ES), after which RIN was measured with a fast-Fourier-transformer (Stanford, SR785) by analyzing the output of the photodetector. Figure 2B shows the RIN curves of the two frequency combs [comb1 (blue) and comb2 (red)] at a pump power of 670 mW. The noise level was estimated to be 120 dBc/

Hz for low frequencies and then rapidly dropped above 10 kHz, owing to the long relaxation time of Erbium ions leading to the fluctuation suppression in pump light. As a result, the integrated RIN for comb1 and comb2 was calculated to be 0.033% and 0.032%, respectively. Owing to the almost identical integrated RIN between the two frequency combs, we observed almost no difference in RIN noise levels between the fast-axis and slow-axis operative lasers.

The RF spectra from 0 to 500 MHz of the two frequency combs measured using a signal and spectrum analyzer (ROHDE&SCHWAEZ, FSW) are shown in Figure 3A [comb1 (upper) and comb2 (lower)]. We obtained a high signal-to-noise ratio (SNR) of f_{rep} with more than 80 dB at a resolution bandwidth (RBW) of 100 kHz, a fundamental f_{rep} of 82.01 MHz for the two frequency combs, and a Δf_{rep} of ~ 2 kHz between the two frequency combs, respectively. Δf_{rep} might have slight fluctuation owing to the fluctuations of environmental temperature and pump power. We also observed that the fluctuation of f_{rep} in a fiber laser was sub-kilohertz magnitude due to environmental perturbations in the free-running operation. Hence, to evaluate the influence of environmental perturbations on f_{rep} in two outputs of dual-comb fiber laser, temporal variations in f_{rep} were measured using two frequency counters (Tektronix, 53,230). Figure 3B shows the temporal f_{rep} changes of the outputs [comb1 (blue) and comb2 (red)]. Notably, a change of ~ 300 Hz was observed in f_{rep} due to temperature variations. Next, the frequency instability of



Δf_{rep} was measured by mixing the two f_{rep} RF signals, and after which Δf_{rep} was extracted using a low-pass filter before being recorded by a frequency counter. The frequency jitter of Δf_{rep} for the laser *versus* time (for a gating time of 2 m) is shown in Figure 3C. We observed a standard deviation of 1.59 Hz at Δf_{rep} of 2.09 kHz. Therefore, the non-aliasing bandwidth of the laser was calculated to be ~ 1.6 THz. Figure 3D shows the Allan deviation of Δf_{rep} , which was about 8.2×10^{-4} at 0.002 s, rolling down to 9.1×10^{-6} at 10 s with a slope of $1/\tau^{1/2}$. A ~ 42 kHz accuracy could be provided by this uncertainty on optical frequency domain. Compared with the fluctuation (~ 300 Hz) of f_{rep} in each comb, high relative stability was obtained for Δf_{rep} with an Allan deviation of 0.05 Hz for an averaging time of 1 s without servo control. An enormous improvement in relative stability was found, owing to sharing of the NALM part. This improvement had effective advantages in DCS, where constant Δf_{rep} is required during multi-heterodyne beating. Still, due to environmental perturbations, the Allan deviation curve of Δf_{rep} turned up after 10 s, which could be effectively improved in the long term by employing temperature control.

The relative coherence between the two frequency combs of the dual-comb fiber laser at the same center wavelength was evaluated using a narrow-linewidth single-frequency continuous wave (CW) laser (NKT Photonics, Koheras BASIK, E15) with a very narrow linewidth of <0.1 kHz at

1,555.5 nm. We separately combined the two frequency combs with the CW laser and the band-pass filter extracted the two beat signals. Subsequently, the two beat notes were mixed after amplifying, after which the relative beat note was extracted by filtering. The RF spectra of the beat notes are shown in Figures 4A, B. We obtained a high SNR of the beat notes with more than 30 dB at an RBW of 100 kHz, indicating that each frequency comb from the dual-comb fiber laser had a high coherence with the CW laser at 1,555.5 nm. Additionally, due to the low extinction ratio devices used in the laser cavity, a small polarization crosstalk was also observed in Figures 4A, B, which could be further suppressed by employing the higher extinction ratio devices. Figure 4C shows the relative beat note between the two frequency combs at 1,555.5 nm (for a measurement time of 4.19 ms). The linewidth of the relative beat note was ~ 1 kHz (RBW = 300 Hz), indicating that the two frequency combs from this dual-comb fiber laser configuration had high mutual coherence.

4 Conclusion

To develop a practical source, this study has developed a polarization-multiplexed, Er-doped dual-comb fiber laser based on an all-PM cavity configuration. Notably, NALM with a non-

reciprocal phase shifter was used for the passive and low-noise mode-locking operation. As a result, while the FWHM bandwidth of the two frequency combs was ~ 13.0 nm at $\sim 1,563$ nm, the f_{rep} was measured to be 82.01 MHz. Furthermore, while the standard deviation was 1.59 Hz at Δf_{rep} of 2.09 kHz, the FWHM of the relative beat note was ~ 1 kHz without servo control. Hence, this simple, robust, turnkey laser configuration with high relative stability and mutual coherence can be a promising tool in practical DCS. In the future, the stability can be further improved by employing a precision temperature control and using micro-optic package to integrate free-space setups. Moreover, this laser can also be applied to a broad range of fast measurements based on a dual-comb system.

Data availability statement

The raw data supporting the conclusion of this article will be made available by the authors, without undue reservation.

Author contributions

BR and ML: optical experiment XY, LY, XC, and RY: electrical experiment SZ and PZ: guidance and revision.

References

- Steinmetz T, Wilken T, Araujo-Hauck C, Holzwarth R, Hnsch TW, Pasquini L, et al. Laser frequency combs for astronomical observations. *Science* (2008) 321: 1335–7. doi:10.1126/SCIENCE.1161030
- Benedick AJ, Chang G, Birge JR, Chen LJ, Kärtner FX, Li CH, et al. Visible wavelength astro-comb. *Opt Express* (2010) 18:19175–84. doi:10.1364/OE.18.019175
- Glenday AG, Li CH, Langellier N, Chang G, Chen LJ, Furesz G, et al. Operation of a broadband visible-wavelength astro-comb with a high-resolution astrophysical spectrograph. *Optica* (2015) 2:250. doi:10.1364/OPTICA.2.000250
- Rubiola E, Santarelli G. The purest microwave oscillations. *Nat Photon* (2013) 7:269–71. doi:10.1038/nphoton.2013.79
- McFerran JJ, Ivanov EN, Bartels A, Wilpers G, Oates CW, Diddams SA, et al. Low-noise synthesis of microwave signals from an optical source. *Electron Lett* (2005) 41:650–1. doi:10.1049/el:20050505
- Kippenberg TJ, Holzwarth R, Diddams SA. Microresonator based optical frequency combs. *Science* (2011) 332:555–9. doi:10.1126/science.1193968
- Adler F, Masowski P, Foltynowicz A, Cossel KC, Ye J, Hartl I, et al. Mid-infrared Fourier transform spectroscopy with a broadband frequency comb. *Opt Express* (2010) 18:21861–72. doi:10.1364/OE.18.021861
- Gohle C, Stein B, Schliesser A, Udem T, Hansch TW. Frequency comb vernier spectroscopy for broadband, high-resolution, high-sensitivity absorption and dispersion spectra. *Phys Rev Lett* (2007) 99:263902–4. doi:10.1103/PhysRevLett.99.263902
- Coddington I, Newbury N, Swann W. Dual-comb spectroscopy. *Optica* (2016) 3:414. doi:10.1364/OPTICA.3.000414
- Salvadé Y, Schuhler N, Lévêque S, Le FS. High-accuracy absolute distance measurement using frequency comb referenced multiwavelength source. *Appl Opt* (2008) 47:2715–20. doi:10.1364/ao.47.002715
- Minoshima K, Matsumoto H. High-accuracy measurement of 240-m distance in an optical tunnel by use of a compact femtosecond laser. *Appl Opt* (2000) 39: 5512–7. doi:10.1364/ao.39.005512
- Sinclair LC, Coddington I, Swann WC, Rieker GB, Hati A, Iwakuni K, et al. Operation of an optically coherent frequency comb outside the metrology lab. *Opt Express* (2014) 22:6996. doi:10.1364/OE.22.006996
- I Hartl, L Dong, Fermann ME, Schibli TR, Onae A, Hong FL, et al. *Long-term carrier envelope phase locking of a PM fiber frequency comb source*. Optical Fiber Communication Conference (2005).
- Sinclair LC, Deschênes J, Sonderhouse L, Swann WC, Coddington I, Baumann E, et al. Invited article: A compact optically coherent fiber frequency comb. *Rev Sci Instrum* (2015) 86:081301. doi:10.1063/1.4928163
- Edelmann M, Hua Y, Safak K, Kaertner FX. Intrinsic amplitude-noise suppression in fiber lasers mode-locked with nonlinear amplifying loop mirrors. *Opt Lett* (2021) 46:1752–5. doi:10.1364/OL.415718
- Raabe N, Feng T, Mero M, Tian H, Song Y, Haensel W, et al. Excess carrier-envelope phase noise generation in saturable absorbers. *Opt Lett* (2017) 42:1068–71. doi:10.1364/OL.42.001068
- Ning K, Hou L, Fan ST, Yan LL, Zhang YY, Rao BJ, et al. An all-polarization-maintaining multi-branch optical frequency comb for highly sensitive cavity ring-down spectroscopy. *Chin Phys Lett* (2020) 37:064202. doi:10.1088/0256-307X/37/6/064202
- Hansel W, Hoogland H, Giunta M, Schmid S, Steinmetz T, Doubek R, et al. All polarization-maintaining fiber laser architecture for robust femtosecond pulse generation. *Appl Phys B* (2017) 123:41. doi:10.1007/s00340-016-6598-2
- Kuse N, Jiang J, Lee CC, Schibli TR, Fermann ME. All polarization-maintaining Er fiber-based optical frequency combs with nonlinear amplifying loop mirror. *Opt Express* (2016) 24:3095. doi:10.1364/OE.24.003095

Funding

This work is supported by the Strategic Priority Research Program of the Chinese Academy of Sciences (Grant No. XDB35030101), the Quantum Control and Quantum Information of the National Key Research and Development Program of China (Grant No. 2020YFA0309800), the National Natural Science Foundation of China (Grant No. 12103060), the West Light Foundation of the Chinese Academy of Sciences (XAB2019B19).

Conflict of interest

The authors declare that the research was conducted in the absence of any commercial or financial relationships that could be construed as a potential conflict of interest.

Publisher's note

All claims expressed in this article are solely those of the authors and do not necessarily represent those of their affiliated organizations, or those of the publisher, the editors and the reviewers. Any product that may be evaluated in this article, or claim that may be made by its manufacturer, is not guaranteed or endorsed by the publisher.

20. Keilmann F, Gohle C, Holzwarth R. Time-domain mid-infrared frequency-comb spectrometer. *Opt Lett* (2004) 29:1542–4. doi:10.1364/ol.29.001542
21. Schiller S. Spectrometry with frequency combs. *Opt Lett* (2002) 27:766. doi:10.1364/ol.27.000766
22. Newbury NR, Coddington I, Swann W. Sensitivity of coherent dual-comb spectroscopy. *Opt Express* (2010) 18:7929–45. doi:10.1364/OE.18.007929
23. Coddington I, Swann W, Newbury N. Coherent dual-comb spectroscopy at high signal-to-noise ratio. *Phys Rev A (Coll Park)* (2010) 82:043817–7. doi:10.1103/PhysRevA.82.043817
24. Coddington I, Swann WC, Newbury NR. Coherent multiheterodyne spectroscopy using stabilized optical frequency combs. *Phys Rev Lett* (2008) 100:013902. doi:10.1103/PhysRevLett.100.013902
25. Sean C, Alden CB, Robert W, Kevin C, Esther B, Gar-Wing T, et al. Regional trace-gas source attribution using a field-deployed dual frequency comb spectrometer. *Optica* (2018) 5:320. doi:10.1364/OPTICA.5.000320
26. Xin Z, Zheng L, Liu Y, Liu L, Jiang Y, Yang X, et al. Switchable, dual-wavelength passively mode-locked ultrafast fiber laser based on a single-wall carbon nanotube modelocker and intracavity loss tuning. *Opt Express* (2011) 19:1168–73. doi:10.1364/OE.19.001168
27. Xing L, Tong HT, Saini TS, Nguyen H, Ohishi Y. Tunable and switchable all-fiber dual-wavelength mode locked laser based on Lyot filtering effect. *Opt Express* (2019) 27:14635. doi:10.1364/OE.27.014635
28. Xin Z, Hu G, Zhao B, Cui L, Zheng Z, Liu Y, et al. Picometer-resolution dual-comb spectroscopy with a free-running fiber laser. *Opt Express* (2016) 24:21833–45. doi:10.1364/OE.24.021833
29. Mehrahar S, Norwood RA, Peyghambarian N, Kieu K. Real-time dual-comb spectroscopy with a free-running bidirectionally mode-locked fiber laser. *Appl Phys Lett* (2016) 108:231104. doi:10.1063/1.4953400
30. Xin Z, Zheng Z, Liu Y, Hu G, Liu J. Dual-wavelength, bidirectional single-wall carbon nanotube mode-locked fiber laser. *IEEE Photon Technol Lett* (2014) 26:1722–5. doi:10.1109/lpt.2014.2332000
31. Nakajima Y, Hata Y, Minoshima K. High-coherence ultra-broadband bidirectional dual-comb fiber laser. *Opt Express* (2019) 27:5931. doi:10.1364/OE.27.005931
32. Abdukerim N, Kayes MI, Rezik A, Rochette M. Bidirectional mode-locked thulium-doped fiber laser. *Appl Opt* (2018) 57:7198–202. doi:10.1364/AO.57.007198
33. Zhao X, Ting L, Liu Y, Li Q, Zheng Z. Polarization-multiplexed, dual-comb all-fiber mode-locked laser. *Photon Res* (2018) 6:853–32. doi:10.1364/PRJ.6.000853
34. Nakajima Y, Hata Y, Minoshima K. All-polarization-maintaining, polarization-multiplexed, dual-comb fiber laser with a nonlinear amplifying loop mirror. *Opt Express* (2019) 27:14648. doi:10.1364/OE.27.014648
35. Zhao K, Gao C, Xiao X, Yang C. Buildup dynamics of asynchronous vector solitons in a polarization-multiplexed dual-comb fiber laser. *Opt Lett* (2020) 45:4040–3. doi:10.1364/OL.398323
36. Akosman AE, Sander MY. Dual comb generation from a mode-locked fiber laser with orthogonally polarized interlaced pulses. *Opt Express* (2017) 25:18592–602. doi:10.1364/OE.25.018592
37. Ya L, Xin Z, Guoqing H, Cui L, Bofeng Z, Zheng Z. Unidirectional, dual-comb lasing under multiple pulse formation mechanisms in a passively mode-locked fiber ring laser. *Opt Express* (2016) 24:21392–8. doi:10.1364/OE.24.021392
38. Li R, Tian H, Li Y, Liu B, Song Y, Hu M, et al. All-polarization-maintaining dual-wavelength mode-locked fiber laser based on Sagnac loop filter. *Opt Express* (2018) 26:28302–11. doi:10.1364/OE.26.028302
39. Guo Z, Hao Q, Huang K, Zeng H. All-normal-dispersion mode-locked fiber laser with a tunable angle-spliced polarization-maintaining fiber Lyot filter. *IEEE Photon J* (2021) 13:1–8. doi:10.1109/JPHOT.2021.3079417
40. Fellingner J, Mayer AS, Winkler G, Grosinger W, Truong G-W, Droste S, et al. Tunable dual-comb from an all-polarization-maintaining single-cavity dual-color Yb: Fiber laser. *Opt Express* (2019) 27:28062–74. doi:10.1364/OE.27.028062
41. Nakajima Y, Kusumi Y, Minoshima K. Mechanical sharing dual-comb fiber laser based on an all-polarization-maintaining cavity configuration. *Opt Lett* (2021) 46:5401–4. doi:10.1364/OL.440818
42. Liu X, Liu G, Zhou R, Yu D, Wu J, Fu HY, et al. An all polarization-maintaining fiber laser mode locked by nonlinear amplifying loop mirror with different biases. *Laser Phys* (2020) 30:085104. doi:10.1088/1555-6611/ab964b
43. Li R, Shi H, Wen D, Li Y, Wu Z, Tian H, et al. All-polarization-maintaining erbium-doped mode-locking fiber laser based on nonlinear polarization loop mirror. *Infrared Laser Eng* (2018) 47:0803006. doi:10.3788/IRLA201847.0803006
44. Dudley LM, Barry LP, Harvey JD, Thomson MD, Thomsen BC, Rainer L, et al. Complete characterization of ultrashort pulse sources at 1550 nm. *IEEE J Quan Electron* (1999) 35:441–50. A Publication of the IEEE Quantum Electronics and Applications Society. doi:10.1109/3.753649
45. Zhang Y, Fan S, Yan L, Zhang L, Zhang X, Guo W, et al. Robust optical-frequency-comb based on the hybrid mode-locked Er: fiber femtosecond laser. *Opt Express* (2017) 25:21719–25. doi:10.1364/OE.25.021719
46. Washburn BR, Swann WC, Newbury NR. Response dynamics of the frequency comb output from a femtosecond fiber laser. *Opt Express* (2005) 13:10622–33. doi:10.1364/opex.13.010622
47. Ivanov EN, Diddams SA, Hollberg L. Study of the excess noise associated with demodulation of ultra-short infrared pulses. *IEEE Trans Ultrason Ferroelectr Freq Control* (2005) 52:1068–74. doi:10.1109/TUFFC.2005.1503992